Bull. Mater. Sci., Vol. 37, No. 6, October 2014, pp. 1519–1528. © Indian Academy of Sciences.

In vitro corrosion investigations of plasma-sprayed hydroxyapatite and hydroxyapatite–calcium phosphate coatings on 316L SS

GURPREET SINGH[a],*, HAZOOR SINGH[b] and BUTA SINGH SIDHU[c]

[a]Mechanical Engineering Department, Punjabi University, Patiala 147 002, India
[b]Yadavindra College of Engineering, Punjabi University G.K. Campus, Talwandi Sabo 151 302, India
[c]Punjab Technical University, Jalandhar 144 601, India

MS received 19 March 2013; revised 24 October 2013

Abstract. The present paper discusses various issues associated with biological corrosion of uncoated and plasma-sprayed hydroxyapatite (HA)-coated 316L SS and studies the effect of contents of calcium phosphate (CaP) on corrosion behaviour of hydroxyapatite (HA) coatings in simulated body fluid (Ringer's solution). Three types of coatings, i.e. HA + 20 wt% CaP (type 1), HA + 10 wt% CaP (type 2), HA (type 3), were laid on 316L SS using plasma-spraying technique. Structural characterization techniques including X-ray diffraction (XRD), scanning electron microscopy (SEM) and energy dispersive X-ray spectroscopy (EDX) were used to investigate the crystallinity, microstructure and morphology of the coatings. Electrochemical potentiodynamic tests were performed to determine the corrosion resistance of uncoated and all the three coatings. After the electrochemical corrosion testing, the samples were examined by XRD, SEM and EDX. The electrochemical study showed a significant improvement in the corrosion resistance after HA coating and corrosion resistance of type 3 coating was found maximum.

Keywords. Hydroxyapatite (HA); calcium phosphate (CaP); corrosion; 316L SS.

1. Introduction

The field of biomaterials is of immense importance for mankind, apart from people with diseases, young and dynamic people like sportspersons often need replacements due to fracture and excessive strain. The first and foremost requirement for the choice of the biomaterial to be placed in the human body is that it should be biocompatible and not cause any adverse reaction in the body like allergy, inflammation and toxicity either immediately after surgery or under post-operative conditions (Fraker 1990). Second, biomaterials should possess sufficient mechanical strength and high fracture toughness to sustain the forces of high-load-bearing bones such as femoral and tibia bones, so that they do not undergo fracture (Kokubo *et al* 1999; Kato *et al* 2000). Third and most important consideration is that a bioimplant should have very high corrosion resistance because it will remain intact for a longer period in highly corrosive body environment, which includes blood and other constituents of the body fluid like water, sodium, chlorine, proteins, plasma and amino acids (Lawrence *et al* 1925). Moreover, corrosion can adversely affect the biocompatibility and mechanical properties of the implant.

The dissolution of the surface oxide film and corrosion are the two main factors for introducing additional ions into the body that result in adverse biological reactions leading to mechanical failure of the device (Davis 2003). The composition of the surface oxide film depends on the reactions between the surfaces of metallic materials and living tissues. The dissolution of surface oxide film due to low concentration of dissolved oxygen, inorganic ions, proteins and cells can accelerate the metal ion release (Kasemo and Lausmaa 1986). So, it implies that surface oxide films existing on metallic materials play a significant part, not only for corrosion resistance but also for tissue compatibility. It is recommended to use the corrosion-resistant materials or perform the coating on the implant material to keep the metal ion release at a minimum.

The corrosion resistance of the material is reduced because carbon forms carbides at the grain boundaries. So, the material with low carbon content (<0·030%) such as 316L stainless steel is usually used for manufacturing the surgical implants (Hanawa 2002). The reason for its popularity is relative low cost, reasonable corrosion resistance, increased mechanical strength and ease of fabrication (Songur *et al* 2009; Manivasagam *et al* 2010). But, these steels are subjected to attack when they are transplanted in highly aggressive human body environment (Aksakal *et al* 2010). It has been reported in the literature that 70% of failures in the 316L SS are due to corrosion (Mudali *et al* 2003).

*Author for correspondence (gurpreetsnabha@yahoo.com)

So, to enhance the corrosion resistance and bone-bonding ability of the implant material like biological steel and titanium, coating of bioactive materials such as hydroxyapatite [$(Ca_{10}(PO_4)_6(OH)_2)$, HA] and calcium phosphate is performed (Furlong and Osborn 1991; Kim *et al* 1997; Deligianni *et al* 2001; Hanawa 2002). Various *in vitro* and *in vivo* studies have been carried out to check the clinical success of material for their use as surgical implants. *In vitro* studies are performed to give an overview of the behaviour of the material in simulated body fluid such as Hank's solution or Ringer's solution. The *in vivo* tests that are performed on animal models evaluate the actual performance of the materials as per the standards and guidelines approved by FDA (Food and Drug Administration, USA). Furlong and Osborn, who were the first to perform the clinical trials of HA-coated implants, have reported that HA coatings can successfully enhance clinical success. Delecrin *et al* (1994) have reported that calcium phosphate (CaP) coatings promote early bone apposition at the surface of cementless orthopedic prostheses (D'Antonio *et al* 1996) and have given successful clinical results (Hardy *et al* 1994; Geesink and Hoefnagels 1995; Donnelly *et al* 1997; Dorr *et al* 1998; Hardy *et al* 1999; McNally *et al* 2000).

There are several techniques for depositing the powder on the substrate such as thermal spraying (Gross and Berndt 1998; Gross *et al* 1998; Li *et al* 2002; Chen *et al* 2005; Hao *et al* 2006; Hijon *et al* 2006), sputter coating (Wolke *et al* 2003; Yunzhi *et al* 2005; Thian *et al* 2005), pulsed laser ablation (Cleries *et al* 2000; Zeng and Lacefield 2000; Fernandez-Pradas *et al* 2001; Zhang and Cheng 2011), dynamic mixing (Yoshinari *et al* 1994), dip coating (Shi *et al* 2002; Choi *et al* 2003; Hijon *et al* 2006), sol–gel (Liu *et al* 2002; Manso *et al* 2002; Zhang *et al* 2007), electrophoretic deposition (Manso *et al* 2000; Nie *et al* 2001; Sena *et al* 2002; Ma *et al* 2003; Aniket and Ahmed 2011; Mihai *et al* 2011; Vasilescu *et al* 2011), biomimetic coating (Habibovic *et al* 2002; Adriana *et al* 2008), and hot isostatic pressing (Wie *et al* 1998). Yet plasma spray process is the most commercially, well-preferred technique to deposit HA and CaP on metallic implants because of high deposition rate and a sufficiently low cost (Herman 1988; Ong and Chan 1999; Yang and Chang 2001; Gu *et al* 2002; Chen *et al* 2005).

In this work, atmospheric plasma spray technique was employed to spray HA–CaP coatings on 316L SS substrate. The as-sprayed coatings were characterized by X-ray diffraction (XRD), scanning electron microscopy (SEM) and energy-dispersive X-ray spectroscopy (EDX) techniques. The corrosion behaviour of uncoated, HA- and HA–CaP-coated surgical steel 316L SS (L means low carbon content) in simulated body fluid (Ringer's solution) by conducting the Tafel extrapolation test has been investigated. This study is focused on the effects of adding CaP in HA on the corrosion resistance of HA–CaP coatings. The changes in the crystallinity and morphology of any of the exposed samples were analysed by XRD, SEM and EDX.

2. Experimental

2.1 *Materials*

The medical-grade HA and CaP powders (IFGL Bio Ceramics Limited, Kolkata, India) of 57–200 μm average particle size used as spraying materials. The mixture of HA and CaP powders in composition of HA + 10 wt% CaP and HA + 20 wt% CaP powders were prepared by mechanically stirring the mixture in a ceramic pot for 30 min. Surgical steel 316L SS with chemical composition (in wt%) – C: 0·013; Cr: 17·4; Ni: 10·8; Mo: 2·18; Si: 0·55; Mn: 0·76; P: 0·025; Cu: 0·22; and Fe: balance was used as substrate. Specimens of 316L SS of size $15 \times 15 \times 3$ mm were coated with three different types of coatings: HA + 20 wt% CaP coating (type 1), HA + 10 wt% CaP (type 2) and HA (type 3) using plasma spray (Miller Spray System) at Anod Plasma, Kanpur, India. The substrate surface was grit-blasted with alumina of particle size 50–60 μm at a pressure of 5 bar for 2 min to roughen the surface and subsequently air-blasted to remove any residual grit before spraying. Because a highly roughened substrate surface exhibited higher bond strength as compared to a smooth substrate surface (Nimb *et al* 1993). The plasma spray was performed at 500 A arc current and 50 V arc voltage. The argon, which is the primary gas, was supplied at 57 slpm (standard litre per minute) and the flow rate of secondary gas, hydrogen was 8 slpm. The powder was flown at 11 slpm and the spraying distance between the plasma torch and substrate was 75 mm.

2.2 *Characterization of coatings*

The phase structure of both feedstock powders and all the three coatings was analysed by XPERT-PRO X-ray diffractometer system. In the phase analysis, the radiation source was Cu$K\alpha$; the operating generator setting was 45 kV/40 mA. The feedstock powder and coated samples were scanned over the 2θ range of 10–60° and 25–50°, respectively. Microstructural investigation was carried out on the surfaces and polished cross sections of the coatings by SEM (EVO MA 15 ZEISS) coupled with EDX. As-sprayed coatings were cut with a low-speed precision saw at 75 rpm speed and mounted in hot resin using a hot mounting press, followed by polishing with emery papers of 220, 320, 400, 600, 800, 1000 and 2000 grades, and finally mirror finished by buffing, using an alumina slurry solution on napped cloth. To achieve the desired conductivity for observation in SEM, gold plating were performed on samples. Elemental analysis of the coatings was carried out using an EDX to investigate the Ca/P

ratio and to display the distribution of elements in the coatings.

2.3 *Surface roughness*

Roughness parameters such as R_a (the arithmetic mean of the departures of the roughness profile from the mean line), R_q (root mean square (RMS) of average roughness) and R_z (average of the highest peaks and the lowest valleys) are measured at five different positions on the surface of the uncoated, type 1, type 2 and type 3 coatings on 316L SS specimens by using a roughness tester (SJ-201 MITUTOYO), with a filter of Gaussian type for a cut-off wavelength of 0·8 mm. The average value of each parameter at various positions is reported in this study.

2.4 *Electrochemical corrosion studies*

The electrochemical corrosion behaviour of the uncoated, type 1, type 2 and type 3 coatings on 316L SS was investigated by conducting the potentiodynamic polarization tests. In a potentiodynamic scan, the potential of a metal specimen is slowly swept over a very wide potential range. During the sweep, the metal sample may undergo different electrochemical reactions, resulting in anodic and cathodic cell currents which may vary over many orders of magnitude. Potentiostat/Galvanostat (Series G-750; Gamry Instruments, Inc, USA), interfaced with a personal computer installed with specific Gamry electrochemical software 'DC105', was used to conduct the test. Ringer's solution (Nice Chemical Pvt. Ltd., Cochin, India) with chemical composition (in g/L) as 9 NaCl, 0·24 CaC_{l2}, 0·43 KCl and 0·2 $NaHCO_3$ at pH 7.2 was used as the electrolyte for simulating human body fluid conditions. The 316L SS specimen forms the working electrode. All the potentials were measured with respect to the saturated calomel electrode (SCE) as reference electrode. A graphite rod served as the counter electrode. The instrument measures and controls the potential difference between a non-current-carrying reference electrode and one of the two current-carrying electrodes (the working electrode). All tests were performed at a scan rate of 1 mV/s and fresh solution was used for each experiment. Polarization curves were initiated at –250 to +250 mV relative to open circuit potential. The initial delay of 24 h is given for the stabilization of immersed specimen in Ringer's solution.

3. Results and discussion

3.1 *XRD analysis*

The feedstock powders (HA and CaP) and all the three coated samples were scanned over the 2θ range of 10–60° and 25–50°, respectively. The XRD patterns of HA powder (figure 1) and CaP powder (figure 2) are composed of crystalline phases. All the major peaks belong to HA and CaP matches the JCPDS cards 74-566 and 70-364, respectively. XRD patterns of plasma-sprayed type 1, type 2 and type 3 plasma coating on 316L are shown in figure 3. The structure of all the coatings is crystalline. However, the degree of crystallinity is increasing and the peaks became sharper and less broadened as the presence of calcium phosphate content increased. The rise in peaks of type 1 and type 2 has been noticed in the range of 20° 2θ–25°2θ.

3.2 *SEM/EDX analyses*

3.2a *Surface analysis*: The morphology of HA and CaP powders (figure 4) confirms that the HA powder has the spherical shape and CaP powder has the angular and irregular shape. The size distribution range in both the powders seems to be wider. It is worthwhile to mention

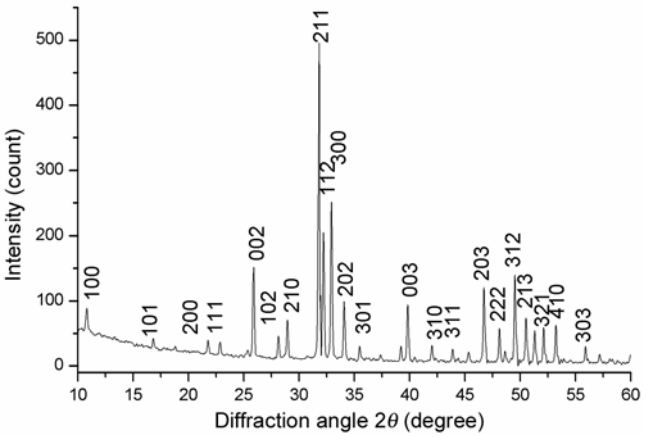

Figure 1. X-ray diffraction patterns of HA powder.

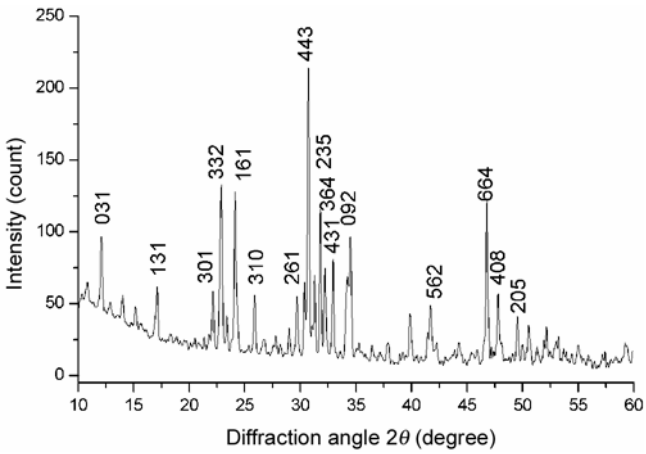

Figure 2. X-ray diffraction patterns of CaP powder.

that the particles size and shape influence the final microstructure of the plasma-spray coating. The morphology and elemental compositions of the surface of type 1, type 2 and type 3 coatings on 316L substrate is investigated by SEM and EDX analyses. SEM micrograph at the surface of type 1 coating (figure 5a) shows the microstructure that consists of well-formed interconnected splats of HA particles with uneven surface. Some voids or pores can also be observed but no microcracks were observed on the coating. The EDX analysis shows the presence of calcium (Ca), phosphorous (P), carbon (C) and oxygen (O) elements, which were main components of HA powder. The average Ca/P ratio was 1·6, which lies in between the guidelines described by the Food and Drug Administration and the ISO standards (FDA 1992; ISO 1996).

SEM micrograph of type 2 coating (figure 5b) shows that the microstructure consist of molten splats which are fused to each other due to the presence of irregular-shaped CaP particles. The coating surface was uneven and some voids were observed, which were less when compared to the type 1 coating. The microstructure of type 3 coatings (figure 5c) appears to be denser and smoother as compared to type 1 and type 2 coatings because of the absence of irregular-shaped CaP particles that lead to the rise in the flattening ratio of the melting particles. It is generally believed that if the density of coating surface is higher then the corrosion resistance of the surface is more. The EDX analysis at three different positions indicates the presence of Ca, P and O. The average value of the Ca/P ratio in type 1 and type 2 coatings were also increased but will remain in agreement with the standard results (FDA 1992; ISO 1996).

3.2b *Cross-sectional analysis*: The characterization of plasma-sprayed type 1, type 2 and type 3 coatings at cross section is performed by SEM and EDX analyses and is shown in figure 6. The average thickness of all the coatings is $100 \pm 20\ \mu$m. All the coatings show good bond with the substrate. The type 1 and type 2 coatings (figure 6a,b) have significant presence of pores. The analysis reveals that type 1 coating (figure 6c) appears to be denser and smoother. The EDX analysis showed peaks of calcium and phosphor are longer in type 1 coating in comparison with type 2 and type 3 coatings, because of the mixing of CaP in the HA used as feedstock powder. The increase in proportion of CaP promotes osteoconduction, while HA particles carry the biological apatite precipitation (Daculsi *et al* 1989). It has been reported in

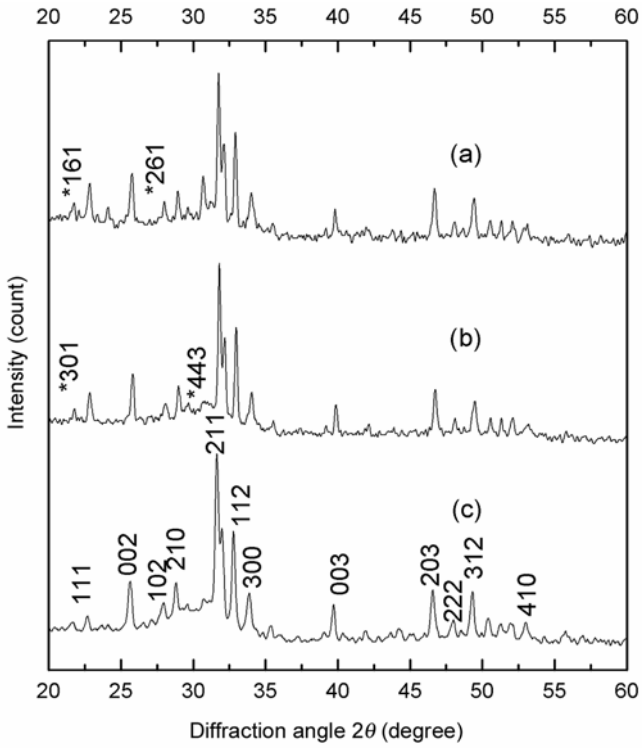

Figure 3. X-ray diffraction pattern of: (**a**) HA + 20 wt% CaP (type 1), (**b**) HA + 10 wt% CaP (type 2) and (**c**) HA (type 3) as-sprayed plasma coatings on 316L SS.

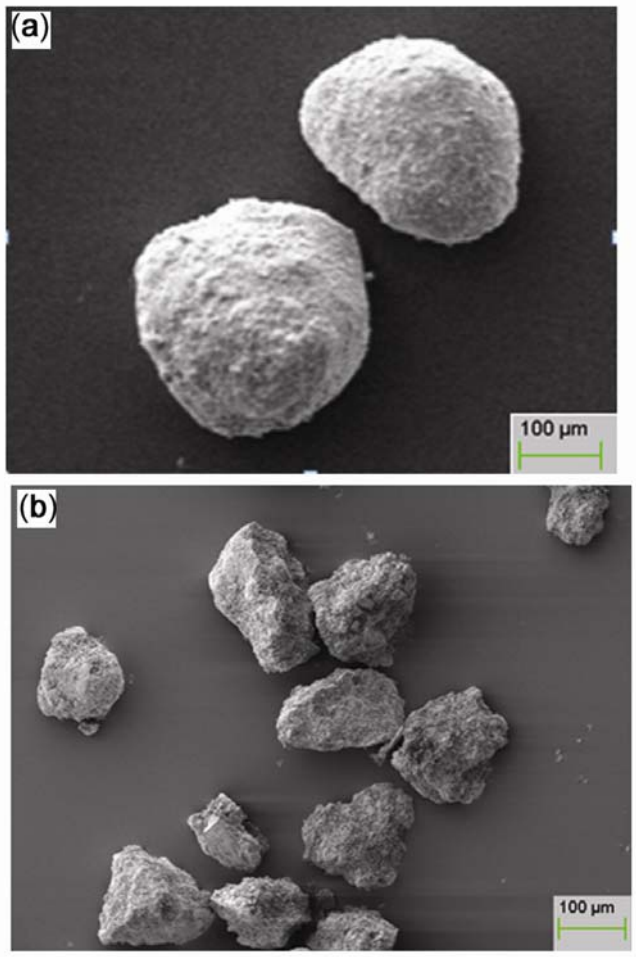

Figure 4. SEM micrograph of (**a**) HA powder and (**b**) CaP powder.

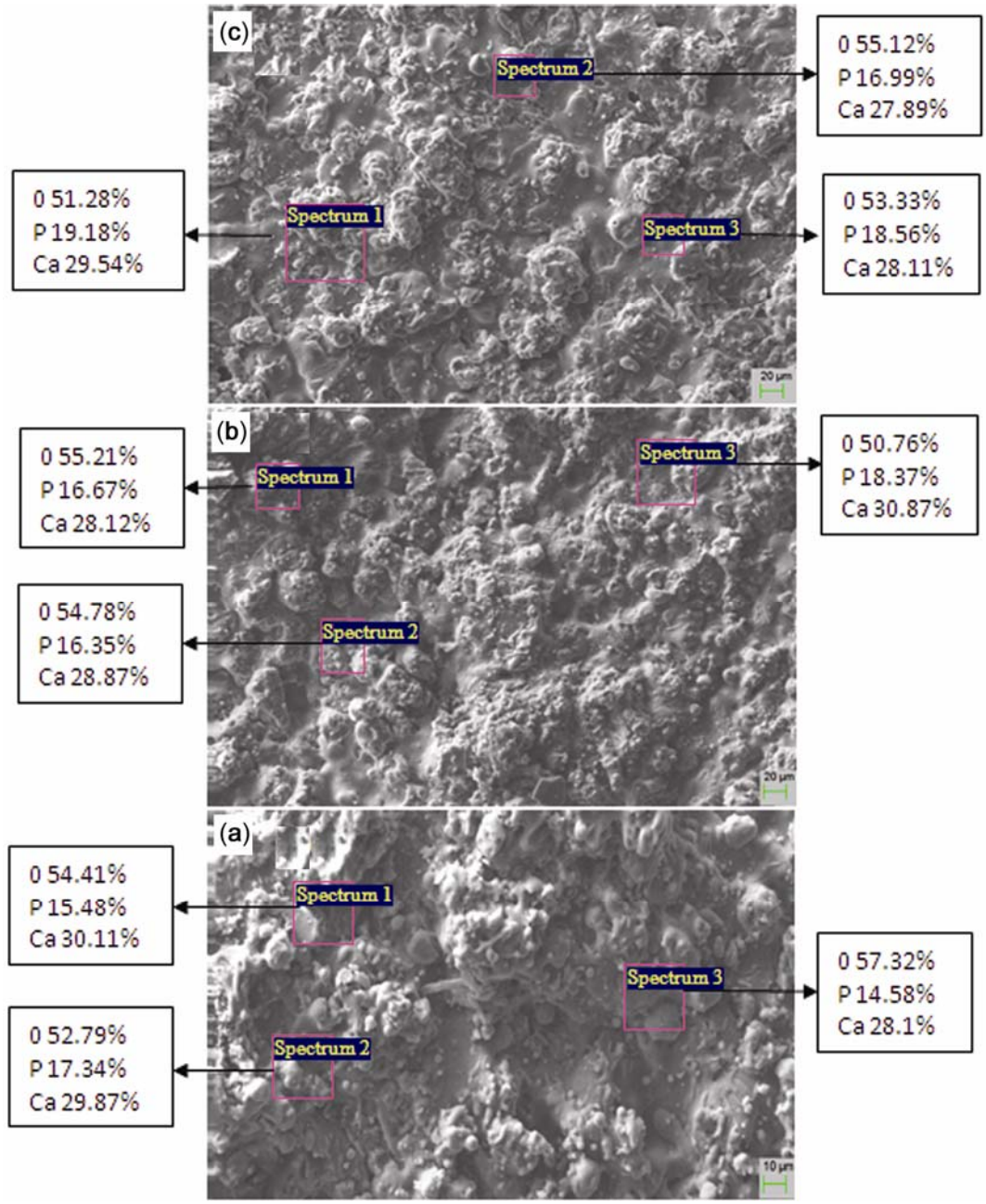

Figure 5. SEM micrograph and EDX analysis at the surface of (**a**) HA + 20 wt% CaP (type 1), (**b**) HA + 10 wt% CaP (type 2) and (**c**) HA (type 3) as-sprayed plasma coatings on 316L SS (*represents the *hkl* indexing of CaP and other represents *hkl* indexing of HA).

literature that highly soluble coatings are more osteoconductive and bioactive in comparison to the stable layers *in vivo* (Dhert *et al* 1993). The osteointegration of CaP coatings is faster than of HA coatings in non-load-bearing conditions (Delecrin *et al* 1994).

3.3 *Surface roughness*

The implant tissue interaction and the biocompatibility in clinical use have been greatly affected by surface roughness, surface topography, surface energy and chemical composition, as reported in literature (Schwartz and Boyan 1994; Lee *et al* 2002). High surface roughness will increase the coating and body-fluid interface, and thus increase the dissolution rate and apatite precipitation (Sun *et al* 2001). The surface roughness parameters (R_a, R_q, and R_z) for uncoated, type 1, type 2 and type 3 plasma coatings on 316L SS are shown in table 1. The average surface roughness (R_a) value for uncoated, type 1, type 2 and type 3 plasma coatings on 316L SS are

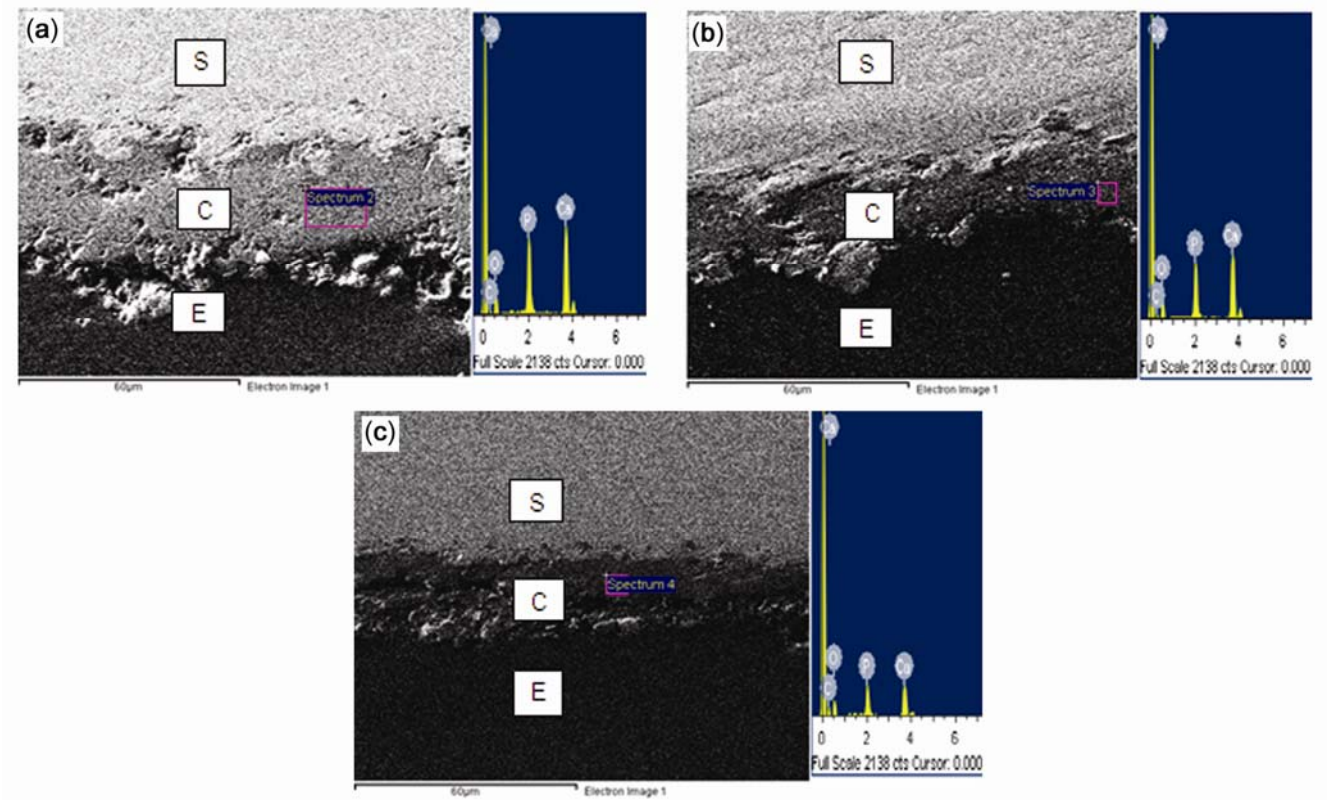

Figure 6. SEM and EDX along the cross section of plasma-sprayed (**a**) HA + 20 wt% CaP (type 1), (**b**) HA + 10 wt% CaP (type 2) and (**c**) HA (type 3) as-sprayed plasma coatings on 316L SS (S, C, E represent the substrate, coating and epoxy, respectively).

Table 1. Roughness values of uncoated 316L SS, type 1, type 2 and type 3 plasma coatings on 316L SS.

Parameter	Uncoated	Type 1 coating	Type 2 coating	Type 3 coating
R_a	0·764	7·2	6·904	5·584
R_z	4·129	40·132	36·79	38·628
R_q	0·968	8·776	8·386	7·186

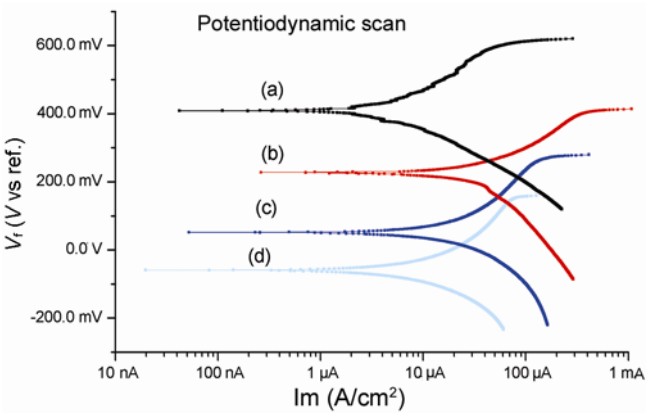

Figure 7. Potentiodynamic curves of (**a**) uncoated, (**b**) HA + 20 wt% CaP (type 1), (**c**) HA + 10 wt% CaP (type 2) and (**d**) HA (type 3) coatings on 316L SS during 24 h immersion in Ringer's solution.

0·764 ± 0·2, 7·2 ± 0·4, 6·904 ± 0·4 and 5·584 ± 0·4 μm, respectively.

Gross and Babovic (2002) reported that plasma-sprayed coating with a powder particle size of 20–30 μm gives a surface roughness of 4–6 μm. The surface roughness of type 3 coating is in agreement, as reported by Gross and Babovic, but the surface roughness of the type 1 and type 2 coatings is just more than 6 μm as the powder particles size is more in this work. Plasma-spray technique is well known for creating HA- and CaP-coated surface composed of rough and smooth areas. The un-melted particles produce rough areas within and on the surface of the coating. Crystalline particles spread over the coating surface when the un-molten particle core is not sufficiently strong to fragment upon impact with the substrate (Gross and Babovic 2002). The smooth areas in the coating are the result of melting of the powder.

Table 2. Corrosion parameters determined by the tafel extrapolation test.

Parameter	Uncoated	Type 1 coating	Type 2 coating	Type 3 coating
β_a, e^{-3} V/decade	197·3	41·10	117·8	157·7
β_c, e^{-3} V/decade	339·5	63·30	811·5	124·7
E_{Corr}, mV	–73·10	–93·60	–87·90	–59·0
I_{Corr}, μA	2·950	1·160	1·130	1·09

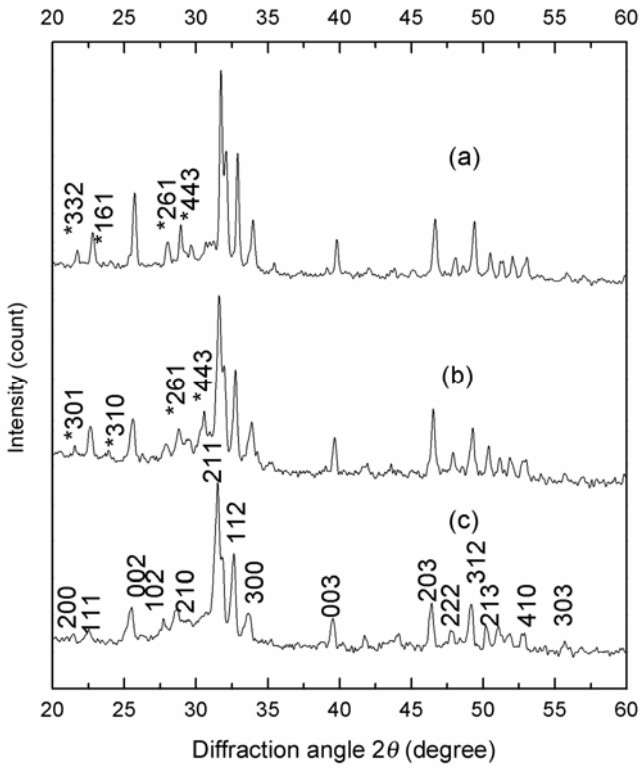

Figure 8. X-ray diffraction pattern of (**a**) HA + 20 wt% CaP (type 1), (**b**) HA + 10 wt% CaP (type 2) and (**c**) HA (type 3) coatings on 316L SS after 24 h immersion in Ringer's solution (* represents the *hkl* indexing of CaP and other represents *hkl* indexing of HA).

3.4 *Corrosion behaviour*

The potentiodynamic scans of the uncoated, type 1, type 2 and type 3 coatings on 316L samples in Ringer's solution are shown in figure 7. The corrosion parameters such as anodic tafel slope (β_a), cathodic tafel slope (β_c), corrosion potential (E_{Corr}) and corrosion current density (I_{Corr}) are determined from the potentiodynamic curves by conducting the tafel extrapolation test. The results of these corrosion parameters are shown in table 2. The chance of corrosion in a material depends upon the corrosion current density (I_{Corr}) at a given potential, material will be more corrosion resistant at a lower value of I_{Corr} (Songur *et al* 2009; Aksakal *et al* 2010; Manivasagam *et al* 2010).

The result of tafel-slope values shows that corrosion current density of type 3 (I_{Corr} = 1·09 μA, E_{Corr} = –59 mV) coating in Ringer's solution is less than the plasma-sprayed type 2 (I_{Corr} = 1·130 μA, E_{Corr} = –87·90 mV) and type 1 (I_{Corr} = 1·160 μA, E_{Corr} = –93·60 mV) coating on 316L SS, whereas the corrosion current density of uncoated 316L SS sample in Ringer's solution is (I_{Corr} = 2·950 μA, E_{Corr} = –73·10 mV) highest.

So the analysis of tafel-slope values indicates that the type 3 coating on 316L SS with lowest I_{Corr} values is the most corrosion-resistant specimen among the uncoated, type 1 and type 2 coated 316L SS specimens in Ringer's solution. The results also suggest that the increase in percentage of CaP in HA also decreases the corrosion resistance of plasma coating 316L SS. The results are in agreement with the previous studies conducted by Singh *et al* 2012, 2013).

After electrochemical corrosion testing in Ringer's solution, the XRD scans of type 1 (figure 8a), type 2 (figure 8b) and type 3 (figure 8c) coatings show interesting behaviour. All the coatings appeared more crystalline and the intensity of XRD peaks were found to be increased. The sharp peaks after immersion indicate the dissolution of the amorphous phases (Sousa and Barbosa 1996). It is reported that amorphous phases are more soluble than crystalline HA, as they encourage the early bone growth (Maxian *et al* 1993). The dissolution was favourable for the early stages of transformation of biological equivalents that act as a mediator between osteoclast and osteoblast differentiation (Xue *et al* 2004). The higher-crystalline coating leads to longer implant life, while some implant manufacturers prefer a faster-dissolving coating to enhance bone growth (Gross and Saber-Samandari 2007). It has been reported in *in vivo* studies that the phase purity, crystallinity and microstructure of HA coatings affect the biological response of HA coating (Yang *et al* 1997). The crystallinity of the coating leads to different dissolution rates *in vivo*. It had been reported in literature that the crystalline HA coatings showed minor signs of degradation, whereas an amorphous HA coating completely disappeared after 24 weeks in goat femurs (Clemens *et al* 1998).

The microstructural investigations on the surfaces of the exposed specimens were examined by SEM and EDX. The morphology of type 1 and type 2 coatings (figure 9(a and b)) changes to flattened particles and looks smooth and denser after exposure to the corrosion testing in Ringer's solution. A comparison of SEM micrographs of the as-sprayed type 3 (figure 5a) and exposed type 3 coating (figure 9c) shows that the coating had retained its

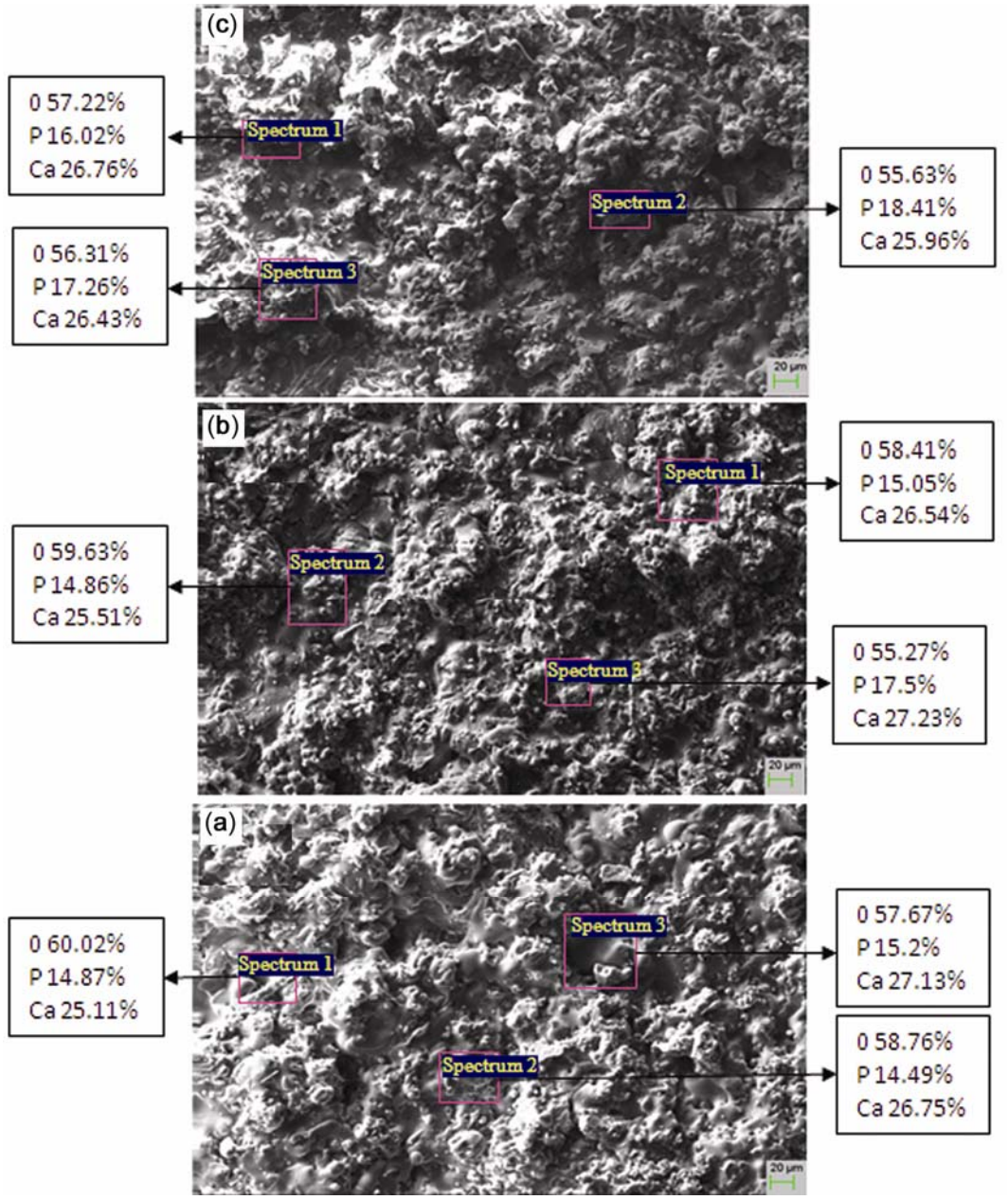

Figure 9. SEM micrograph and EDX analysis at the surface of (**a**) HA + 20 wt% CaP (type 1), (**b**) HA + 10 wt% CaP (type 2) and (**c**) HA (type 3) coatings on 316L SS after 24 h immersion in Ringer's solution.

morphology even after exposure to the corrosion testing. No cracks were found on both the Ha- and HA–CaP-coated exposed specimens.

EDX analysis confirms the presence of Ca, P and O elements in all coatings. EDX analyses of exposed specimens show that Ca and P (at%) decrease by taking the average of elemental composition at three spectra after 24 h immersion in Ringer's solution. The decrease in the values indicates that phosphate accumulates on the surface, which suggests that incongruent dissolution of the HA has taken place (Sousa and Barbosa 1996). No constituent of substrate such as Cr, Ni and Mo was found on the surface of any coatings after immersion for 24 h in Ringer's solution.

4. Conclusions

In the present study, plasma-spray technique was used to deposit the HA + 20 wt% CaP (type 1), HA + 10 wt% CaP (type 2) and HA (type 3) coatings on 316L SS. The plasma-sprayed type 3 and type 2 coatings are more crystalline than type 1 coating on 316L SS. The plasma-sprayed

type 1 and type 2 coatings exhibited higher surface roughness than type 3 coating on 316L SS. The electrochemical study showed the corrosion resistance of the 316L SS increased after the deposition of plasma-sprayed type 3 coating compared to uncoated, type 1 and type 2 plasma-sprayed coatings on 316L SS in Ringer's solution. A comparison of the SEM micrographs of both plasma-sprayed coatings before and after corrosion testing in Ringer's solution showed that HA coating retains its morphology, whereas the morphology of HA + 20 wt% CaP and HA + 10 wt% CaP coatings changes to flattened particles and looks smoother and denser after exposure to the corrosion testing in Ringer's solution. No cracks were found on any coated exposed specimens.

Future *in vivo* studies of plasma-sprayed type 1, type 2 and type 3 coatings on 316L SS and a complete interpretation of these results can help in assessing their use in clinical applications.

References

Adriana Bigi, Milena Fini, Barbara Bracci, Elisa Boanini, Paola Torricelli, Gianluca Giavaresi, Nicolo N, Aldini Alessandro, Facchini Fausto Sbaiz and Roberto Giardino 2008 *Biomaterials* **29** 1730

Aksakal B, Gavgali M and Dikici B 2010 *J. Mater. Eng. Perform.* **19** 894

Aniket and Ahmed El-Ghannam 2011 *J. Biomed. Mater. Res. Part B: Appl. Biomater.* **B99** 369

Chen C, Wang D, Bao Q, Zhang L and Lei T 2005 *Appl. Surf. Sci.* **250** 98

Choi J, Bogdanski D, Koller M, Esenwein S A, Muller D, Muhr G and Epple M 2003 *Biomaterials* **24** 3689

Cleries L, Martinez E, Fernandez-Pradas J M, Sardin G, Esteve J and Morenza J L 2000 *Biomaterials* **21** 967

Clemens J A, Klein C P, Vriesde R C, Rozing P M and Groot K D 1998 *J. Biomed. Mater. Res.* **3** 341

D'Antonio J A, Capello W N and Manley M T 1996 *J. Bone Jt. Surg. Am.* **8** 1226

Daculsi G, LeGeros R Z, Nery E, Lynch K and Kerebel B 1989 *J. Biomed. Mater. Res.* **8** 883

Davis J R 2003 *Handbook of materials for medical devices* (ASM International)

Delecrin J, Daculsi G, Passuti N and Duquet B 1994 *Cells Mater.* **1** 51

Deligianni D D, Katsala N D, Koutsoukos P G and Missirlis Y F 2001 *Biomaterials* **22** 87

Dhert W J, Klein C P, Jansen J A, Van der Velde E A, Vriesde R C and Rozing P M 1993 *J. Biomed. Mater. Res.* **27** 127

Donnelly W J, Kobayashi A, Freeman M A, Chin T W, Yeo H and West M 1997 *J. Bone Jt. Surg. Br.* **3** 351

Dorr L D, Wan Z, Song M and Ranawat A 1998 *J. Arthroplasty* **7** 729

FDA 1992 *Calcium phosphate (Ca–P) coating draft guidance for preparation of FDA submissions for orthopedic and dental endosseous implants* (Washington DC Food and Drug Administration) p. 1

Fernandez-Pradas J M, Cleries L, Martinez E, Sardin G, Esteve J and Morenza J L 2001 *Biomaterials* **22** 2171

Fraker A C 1992 *Corrosion ASM handbook* (ASM International) vol. 13, p. 1324

Furlong R J and Osborn J F 1991 *J. Bone. Jt. Surg.* **B73** 741

Geesink R G and Hoefnagels N H 1995 *J. Bone. Jt. Surg. Br.* **4** 534

Gross K A and Babovic M 2002 *Biomaterials* **23** 4731

Gross K A and Saber-Samandari S 2007 *J. Aust. Ceram. Soc.* **43** 98

Gross K A and Berndt C C 1998 *J. Biomed. Mater. Res.* **39** 580

Gross K A, Berndt C C and Herman H 1998 *J. Biomed. Mater. Res.* **39** 407

Gu Y W, Loh N H, Khor K A, Tor S B and Cheang P 2002 *Biomaterials* **23** 37

Habibovic P, Barrere F, Van Bliterswijk De C A, Groot K and Layrolle P 2002 *J. Am. Ceram. Soc.* **85** 517

Hanawa T 2002 *J. Artif. Organs* **12** 73

Hao Wang, Noam Eliaz, Zhou, Xiangc Hu-Ping and Hsuc Myron 2006 *Biomaterials* **27** 4192

Hardy D C, Frayssinet P, Bonel G, Authom T, Naelou Le and Delince S A PE 1994 *Acta Orthop. Scand.* **3** 253

Hardy D C, Frayssinet P, Krallis P, Descamps P Y, Fabeck L and Delplancke J L 1999 *Acta Orthop. Belg.* **1** 72

Herman H 1988 *MRS Bull.* **12** 60

Hijon N, Victoria Cabanas M, Juan Pena and Vallet Regi Maria 2006 *Acta Biomater.* **2** 567

ISO 1996 *Implants for surgery: coating for hydroxyapatite ceramics* (ISO) p. 1

Kasemo B and Lausmaa J 1986 *CRC Crit. Rev. Biocompat.* **2** 335

Kato H, Nakamura T, Nishiguchi S, Matsusue Y, Kobayashi M, Miyazaki T, Kim H M and Kokubo T 2000 *J. Biomed. Mater. Res.* **53** 28

Kim H M, Miyaji F, Kokubo T and Nakamura T 1997 *J. Biomed. Mater. Res.* **38** 121

Kokubo T, Miyaji F and Kim H M 1999 *J. Am. Ceram. Soc.* **79** 1127

Lawrence S K, Gertrude M and Shults 1925 *J. Exp. Med.* **42** 565

Lee T M, Tsai R S, Chang E, Yang C Y and Yang M R 2002 *J. Mater. Sci.: Mater. Med.* **13** 341

Li H, Khor K A and Cheang P 2002 *Biomaterials* **23** 85

Liu D, Yang Q and Troczynski T 2002 **23** 691

Ma J, Wang C and Peng K W 2003 *Biomaterials* **24** 3505

Manivasagam G, Dhinasekaran D and Rajamanickam A 2010 *Recent Pat. Corros. Sci.* **2** 40

Manso M, Jimenez C, Morant C, Herrero P and Martinez-Duart J M 2000 *Biomaterials* **21** 1755

Manso M, Langlet M, Jimenez C and Martinez-Duart J M 2002 *Biomol. Eng.* **19** 63

Maxian S H, Zawadsky J P and Dunn M G 1993 *J. Biomed. Mater. Res.* **27** 717

McNally S A, Shepperd J A, Mann C V and Walczak J P 2000 *J. Bone Jt. Surg. Br.* **3** 378

Mihai V Popa, Jose Maria Calderon Moreno, Monica Popa, Ecaterina Vasilescu, Paula Drob, Cora Vasilescu and Silviu I Drob 2011 *Surf. Coat. Technol.* **20** 4776

Mudali U K, Sridhar T M and Raj B 2003 *Sadhana* **28** 601

Nie X, Leyland A, Matthews A, Jiang J C and Meletis E I 2001 *J. Biomed. Mater. Res.* **57** 612

Nimb L, Gotfredsen K and Steen J J 1993 *Acta Orthop. Belg.* **59** 333

Ong J L and Chan C N 1999 *Crit. Rev. Biomed. Eng.* **28** 667
Schwartz Z and Boyan B D 1994 *J. Cell. Biochem.* **56** 340
Sena D E LA, Andrade D E MC, Rossi A M and Soares G D A 2002 *J. Biomed. Mater. Res.* **60** 1
Shi D, Jiang G and Bauer J 2002 *J. Biomed. Mater. Res.* (*Appl. Biomater.*) **63** 71
Singh G, Singh H and Sidhu B S 2013 *Surf. Coat. Technol.* **228** 242
Singh T P, Singh H and Singh H 2012 *J. Therm. Spray Technol.* (doi: 10.1007/s11666-012-9782-x)
Songur M, Celikkan H, Gokmese F, Simsek S A, Altun N S and Aksu M L 2009 *J. Appl. Electrochem.* **39** 1259
Sousa S R and Barbosa M A 1996 *Biomaterials* **17** 397
Sun L, Berndt C C, Gross K A and Kucuk A 2001 *J. Biomed. Mater. Res.* (*Appl. Biomater.*) **58** 570
Thian E S, Huang J, Best S M, Barber Z H and Bonfield W 2005 *Biomaterials* **26** 2947
Vasilescu C, Drob P, Vasilescu E, Demetrescu I, Ionita D, Prodana M and Drob S I 2011 *Corr. Sci.* **53** 992
Wie H, Hero H and Solheim T 1998 *Int. J. Oral Maxillofac. Implant.* **13** 837
Wolke J G C, Vander Waerden J P C M, Schaeken H G and Jansen J A 2003 *Biomaterials* **24** 2623
Xue W, Tao S, Liu X, Zheng X B and Ding C 2004 *Biomaterials* **25** 415
Yang C Y, Lin R M, Wang B C, Lee T M, Chang E, Hang Y S and Chen P Q 1997 *J. Biomed. Mater. Res.* **37** 335
Yang Y C and Chang E 2001 *Biomaterials* **22** 1827
Yoshinari M, Ohshiro Y and Derand T 1994 *Biomaterials* **15** 529
Yunzhi Yang, Kyo-Han and Kim Joo L Ong 2005 *Biomaterials* **26** 327
Zeng H and Lacefield W R 2000 *J. Biomed. Mater. Res.* **50** 239
Zhang M Y and Cheng G J 2011 *Nano Biosci.* **10** 177
Zhang S, Wang Y S, Zeng X T, Cheng K, Qian M, Sun D E, Weng W J and Chia W Y 2007 *Eng. Fract. Mech.* **74** 1884